10. J. M. Nam, C. S. Thaxton, C. A. Mirkin, *Science* **301**, 1884 (2003).
11. C. H. Setchell, *J. Chem. Technol. Biotechnol. B Biotechnol.* **35**, 175 (1985).
12. C. Delatour, *IEEE Trans. Magn.* **9**, 314 (1973).
13. D. Fletcher, *IEEE Trans. Magn.* **27**, 3655 (1991).
14. D. R. Kelland, *IEEE Trans. Magn.* **34**, 2123 (1998).
15. G. B. Cotten, H. B. Eldredge, *Sep. Sci. Technol.* **37**, 3755 (2002).
16. G. D. Moeser, K. A. Roach, W. H. Green, T. A. Hatton, P. E. Laibinis, *Am. Inst. Chem. Eng. J.* **50**, 2835 (2004).
17. H. U. Worm, *Geophys. J. Int.* **133**, 201 (1998).
18. R. F. Butler, *Paleomagnetism: Magnetic Domains to Geologic Terranes* (Blackwell Scientific, Boston, 1992).
19. D. Horak, F. Lednicky, E. Petrovsky, A. Kapicka, *Macromol. Mater. Eng.* **289**, 341 (2004).
20. G. F. Goya, T. S. Berquo, F. C. Fonseca, M. P. Morales, *J. Appl. Phys.* **94**, 3520 (2003).
21. A. Hutten *et al.*, *J. Biotechnol.* **112**, 47 (2004).
22. A. Ditsch, S. Lindenmann, P. E. Laibinis, D. I. C. Wang, T. A. Hatton, *Ind. Eng. Chem. Res.* **44**, 6824 (2005).
23. See the supporting material on *Science* Online for supplementary data.
24. W. W. Yu, J. C. Falkner, C. T. Yavuz, V. L. Colvin, *Chem. Commun.* **2004**, 2306 (2004).
25. S. H. Sun, H. Zeng, *J. Am. Chem. Soc.* **124**, 8204 (2002).
26. S. Yean *et al.*, *J. Mater. Res.* **20**, 3255 (2005).
27. K. Butter, P. H. H. Bomans, P. M. Frederik, G. J. Vroege, A. P. Philipse, *Nat. Mater.* **2**, 88 (2003).
28. M. R. Parker, *Phys. Technol.* **12**, 263 (1981).
29. G. Iacob, A. Ciochina, O. Bredetean, *Eur. Cell. Mater.* **3**, 167 (2002).
30. A. R. Muxworthy, *Geophys. J. Int.* **144**, 441 (2001).
31. S. Bucak, D. A. Jones, P. E. Laibinis, T. A. Hatton, *Biotechnol. Prog.* **19**, 477 (2003).
32. R. F. Butler, S. K. Banerjee, *J. Geophys. Res.* **80**, 4049 (1975).
33. J. A. Dearing *et al.*, *Geophys. J. Int.* **124**, 228 (1996).
34. R. D. Ambashta, P. K. Wattal, S. Singh, D. Bahadur, *J. Magn. Magn. Mater.* **267**, 335 (2003).
35. B. I. Haukanes, C. Kvam, *Nat. Biotechnol.* **11**, 60 (1993).
36. G. P. Hatch, R. E. Stelter, *J. Magn. Magn. Mater.* **225**, 262 (2001).
37. G. Liu, J. Wang, J. Kim, M. R. Jan, G. E. Collins, *Anal. Chem.* **76**, 7126 (2004).
38. S. R. Kanel, B. Manning, L. Charlet, H. Choi, *Environ. Sci. Technol.* **39**, 1291 (2005).
39. M. A. Hossain *et al.*, *Environ. Sci. Technol.* **39**, 4300 (2005).
40. L. G. Twidwell, J. McCloskey, P. Miranda, M. Gale, in *Proceedings of the Global Symposium on Recycling, Waste Treatment and Clean Technology Conference*, San Sebastian, Spain, 5 to 9 September 1999 (The Minerals, Metals, and Materials Society, Warrendale, PA, 1999), pp. 1715–1726.
41. Y. Kakihara, T. Fukunishi, S. Takeda, S. Nishijima, A. Nakahira, *IEEE Trans. Appl. Supercond.* **14**, 1565 (2004).
42. A. Chiba *et al.*, *IEEE Trans. Appl. Supercond.* **12**, 952 (2002).
43. U.S. Environmental Protection Agency Arsenic Rule, *Fed. Regist.* **66**, 6976 (22 January 2001) [40 Code of Federal Regulations] (www.epa.gov/safewater/arsenic/regulations.html).
44. We thank NSF for its support of the Center for Biological and Environmental Nanotechnology (EEC-0647452). We also acknowledge with gratitude the Office of Naval Research (N00014-04-1-0003), and the U.S. Environmental Protection Agency Star Program (RD-83253601-0) for funding. C.T.Y. thanks the Robert A. Welch Foundation (C-1349) for a graduate fellowship. D. M. Mittleman provided invaluable help in developing this manuscript. Finally, the authors appreciate the efforts of J. Jones and W. Guo, who provided support for the supporting figures included on *Science* Online.

Supporting Online Material
www.sciencemag.org/cgi/content/full/314/5801/964/DC1
Figs. S1 to S5
Table S1
References

19 June 2006; accepted 20 September 2006
10.1126/science.1131475

Localized Temporal Change of the Earth's Inner Core Boundary

Lianxing Wen

Compressional waves of an earthquake doublet (two events occurring in the South Sandwich Islands on 1 December 1993 and 6 September 2003), recorded at three seismic stations in Russia and Kyrgyzstan and reflected off Earth's inner core boundary, arrived at least from 39 to 70 milliseconds earlier in the 2003 event than in the 1993 event. Such changes indicate that Earth's inner core radius enlarged locally beneath middle Africa by 0.98 to 1.75 kilometers between the times of these two events. Changes of the inner core radius may be explained by either a differential motion of the inner core, assuming that irregularities are present at the inner core boundary and fixed to the inner core, or a rapid growth of the inner core by this amount.

Earth's inner core grows from the solidification of the outer core (*1*). The growth of the inner core releases latent heat and dispels light elements, providing driving forces for the outer core convection (*2*) and power for generating the geodynamo (*3*, *4*). The inner core growth process is thought to be geologically slow (*5*–*10*) and geographically uniform because of the presumed extremely small variation in temperature in the outer core (*11*). Here, I used PKiKP [a compressional wave reflected off the inner core boundary (Fig. 1A)] waveforms of an earthquake waveform doublet discovered by Zhang *et al*. (*12*) to study temporal change of the inner core boundary.

Earthquake waveform doublets are earthquakes occurring at different times but in almost exactly the same location and generating similar waveforms (*12*–*18*). Because the relative travel time and waveform difference between the waveform doublets is sensitive only to the relative change of event location and/or the temporal change of seismic properties, it is powerful to use waveform doublets to study high-resolution relative locations of the earthquakes (*13*–*15*) and to detect temporal change of seismic properties (*12*, *16*–*18*). The similarities of the doublet waveforms also allow accurate travel time measurement to be made. Zhang *et al*. (*12*) reported the existence of 19 waveform doublets in the South Sandwich region over a period of 35 years and showed that the PKP(DF) (PKIKP) phases [a compressional wave propagating through the inner core (Fig. 1A)] are in misalignment to each other between the doublets. Their study provided compelling evidence for the reported temporal changes in PKIKP travel time (*19*–*21*). They further proposed that the observed temporal changes can be explained by an inner core differential motion over a lateral velocity gradient in the inner core (*20*).

I used the best doublet reported in Zhang *et al*. (*12*) (table S1). The doublet consists of two events occurring on 1 December 1993 (event 93) and 6 September 2003 (event 03). I used the observed difference in absolute arrival time of various seismic phases that are not associated with the inner core (non-IC phases) between the doublet to determine the relative location and origin time of the two events. I used event 93 as the master event [i.e., fixed its origin time and location to those reported in the earthquake catalog (table S1)] and searched for the best-fitting relative location and origin time for event 03 that minimize the travel time residuals of the non-IC phases between the two events. I then studied the temporal changes of travel time and waveform of the PKiKP-PKIKP or PKiKP phases between the doublet based on the best-fitting relative hypocenter location and origin time of the two events. To do so, the PKiKP and PKiKP-PKIKP waveforms of the doublet were superimposed on the basis of the relative arrival times of these phases between the doublet, estimated using the best-fitting relative location and origin time of the two events. The PKiKP travel time residuals between the doublet are further calculated by subtracting the predicted relative arrival times of the seismic phases from the measured arrival time differences between the doublet. If the superimposed waveforms are in misalignment between the doublet, or if a travel time residual is larger than the relocation error bar, it would mean that the arrival times of the seismic phases between the doublet cannot be explained by the relative origin time and hypocenter location of the doublet, and these phases exhibit temporal change in time.

The detailed relocation analysis places the doublet within 0.37 km in horizontal space and 0.7 km in depth (*22*). The inferred best-fitting relative origin time and hypocenter location between the doublet yield, for the non-IC phases,

Department of Geosciences, State University of New York at Stony Brook, NY 11794, USA. E-mail: Lianxing.Wen@sunysb.edu

a minimal root mean square travel time residual of 0.016 s and a maximal travel time residual of 0.031 s in the individual stations (fig. S1B) (*22*). The maximal travel time residual in the individual stations (0.031 s) is considered as the relocation error bar.

Superimposed PKiKP-PKIKP waveforms and PKiKP waveforms observed at stations ARU (Arti, Russia), AAK (Ala Archa, Kyrgyzstan), and OBN (Obninsk, Russia) reveal that the PKiKP phases observed at these stations are in misalignment and that they arrived earlier in event 03 than in event 93, even after the travel time differences due to the relative hypocenter position of the two events are taken into account (Fig. 1, B to E). The PKiKP and PKIKP phases recorded at station ARU arrived 0.11 s earlier and the PKIKP phase about 0.04 s earlier in event 03 than in event 93. Moreover, the PKiKP-PKIKP differential travel time was about 0.07 s smaller in event 03 than in event 93 (Fig. 1C). Station AAK is closer, and the separation of the PKiKP and PKIKP phases is not clear, but the later portion of the waveforms (energy primarily associated with the PKiKP phases) is clearly in misalignment and arrived about 0.07 s earlier in event 03 than in event 93, whereas the earlier portion of energy appears to have arrived at about the same time (Fig. 1D). The PKiKP waveforms observed at station OBN exhibit two characteristics: (i) the PKiKP main phases are evidently in misalignment between the two events, with the phase in event 03 arriving about 0.07 s earlier than in event 93 and (ii) the PKiKP coda waves show waveform dissimilarities between the two events (Fig. 1E).

The observed smaller differential PKiKP-PKIKP travel times of about 0.07 s at stations ARU and AAK in event 03 further confirm that the PKiKP travel time residuals were not caused by relative event location or origin time of the doublet but by temporal changes of PKiKP travel time between the occurrences of the two events (*22*). The temporal changes in PKiKP travel time are at least 0.07 s at ARU and AAK, using their PKIKP arrival times as reference, and 0.039 s at OBN taking into account the maximal possible error of relocation, with the PKiKP phases arriving earlier in event 03 than in event 93.

No discernible temporal change of PKiKP travel time is observed for other stations. Superimposed PKiKP-PKIKP or PKiKP waveforms of the doublet recorded at other stations show excellent agreements in both absolute arrival time and differential travel time of the two phases (Fig. 2, A and B). The best-fitting relative location and origin time of event 03, obtained using the arrival times of the non-IC phases, also reduce the travel time residuals of the PKiKP and PKIKP phases within the relocation error bar for all other stations (Figs. 2 and 3). For the data available, the temporal changes in the PKiKP travel times are only observed for the phases recorded at ARU, AAK, and OBN, which sampled a localized region of the inner core boundary beneath middle Africa (Fig. 3).

The temporal changes of travel time for the PKiKP phases recorded at stations ARU, AAK, and OBN between the doublet are not likely to have been caused by temporal changes of seismic properties near the hypocenters or in the mantle (*22*).They indicate a localized change of the inner core radius beneath middle Africa between the occurrences of the doublet. A larger radius would produce an earlier PKiKP arrival, because the PKiKP phase would be reflected at a shallower depth. An inner core radius enlarged by 0.98 to 1.75 km would fit the travel time changes of about 0.039 to 0.07 s observed at stations OBN, ARU, and AAK between 1 December 1993 and 6 September 2003.

The localized change of the inner core radius can be explained by a differential inner core rotation, if the inner core boundary has localized topography (Fig. 4A) or locally deviates away from the equilibrium position with a slope of topography (Fig. 4B). In the former case, the PKiKP phases recorded at OBN, ARU, and AAK may sample the topographically low regions in event 93 and the topographically high regions in event 03 that are moved into the sampling points by the inner core differential motion (Fig. 4A). In the latter case, the PKiKP phases recorded at stations OBN, ARU, and AAK in event 03 may sample relatively elevated positions of the nonequilibrium sloped boundary that is moved eastward by the differential rotation of the inner core (Fig. 4B). For these mechanisms to work, it would also require the localized topography or the nonequilibrium slope to be geographically fixed to the inner core as the inner core differentially rotates.

The localized change of inner core radius can also be explained by a rapid localized growth of the inner core by 0.98 to 1.75 km between the occurrences of the doublet, either in the PKiKP sampling points (Fig. 4C) or in a regional scale beneath middle Africa (Fig. 4D). The position of the inner core boundary is controlled by the temperature and the outer core composition (iron and its companion light elements) (*10*). The localized growth may be caused by something unknown (for example, Earth's magnetic field) or by a regional perturbation of temperature and/or composition near the inner core boundary through mechanisms such as a heterogeneous heat-flow flux at the bottom of the outer core induced near the core-mantle boundary (*23*) or small-scale compositional convection in the top of the inner core (*24*).

Both interpretations indicate that the inner core boundary has irregular topography and that the growth of the inner core and the energy release associated with the growth are not geo-

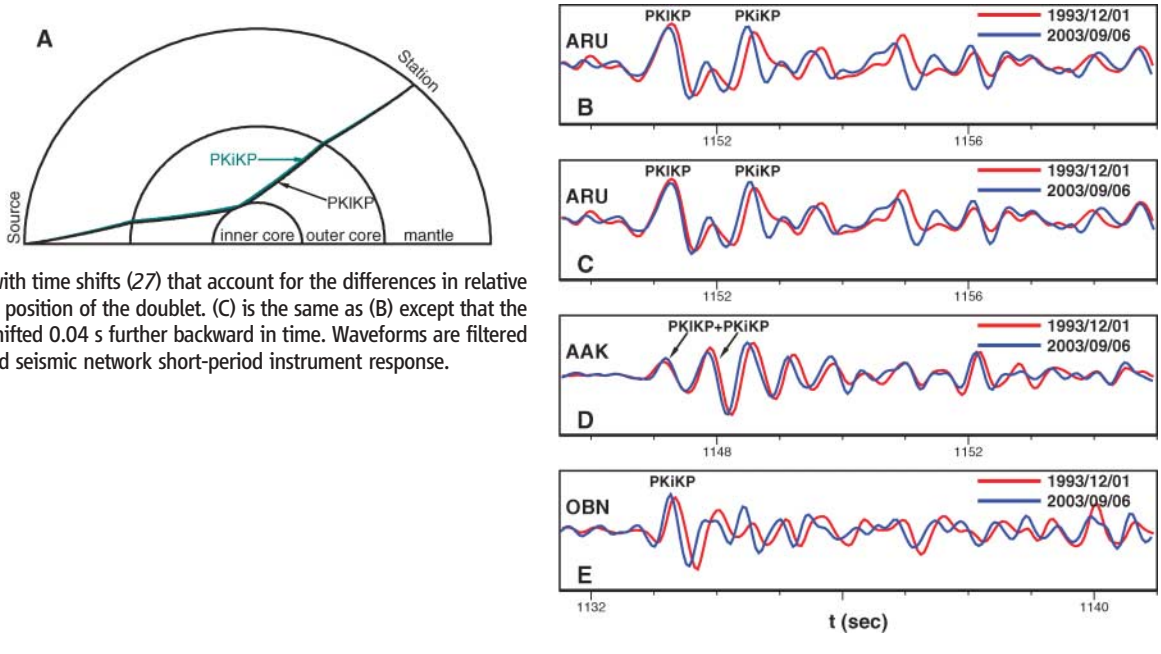

Fig. 1. (**A**) Ray paths of PKIKP (black) and PKiKP (light blue) waves. (**B** to **E**) Superimposed PKiKP-PKIKP waveforms of the doublet recorded at stations ARU (B and C) and AAK (D), and PKiKP waveforms at OBN (E). Waveforms in (B), (D), and (E) are superimposed with time shifts (*27*) that account for the differences in relative origin time and hypocenter position of the doublet. (C) is the same as (B) except that the waveform for event 03 is shifted 0.04 s further backward in time. Waveforms are filtered with the worldwide standard seismic network short-period instrument response.

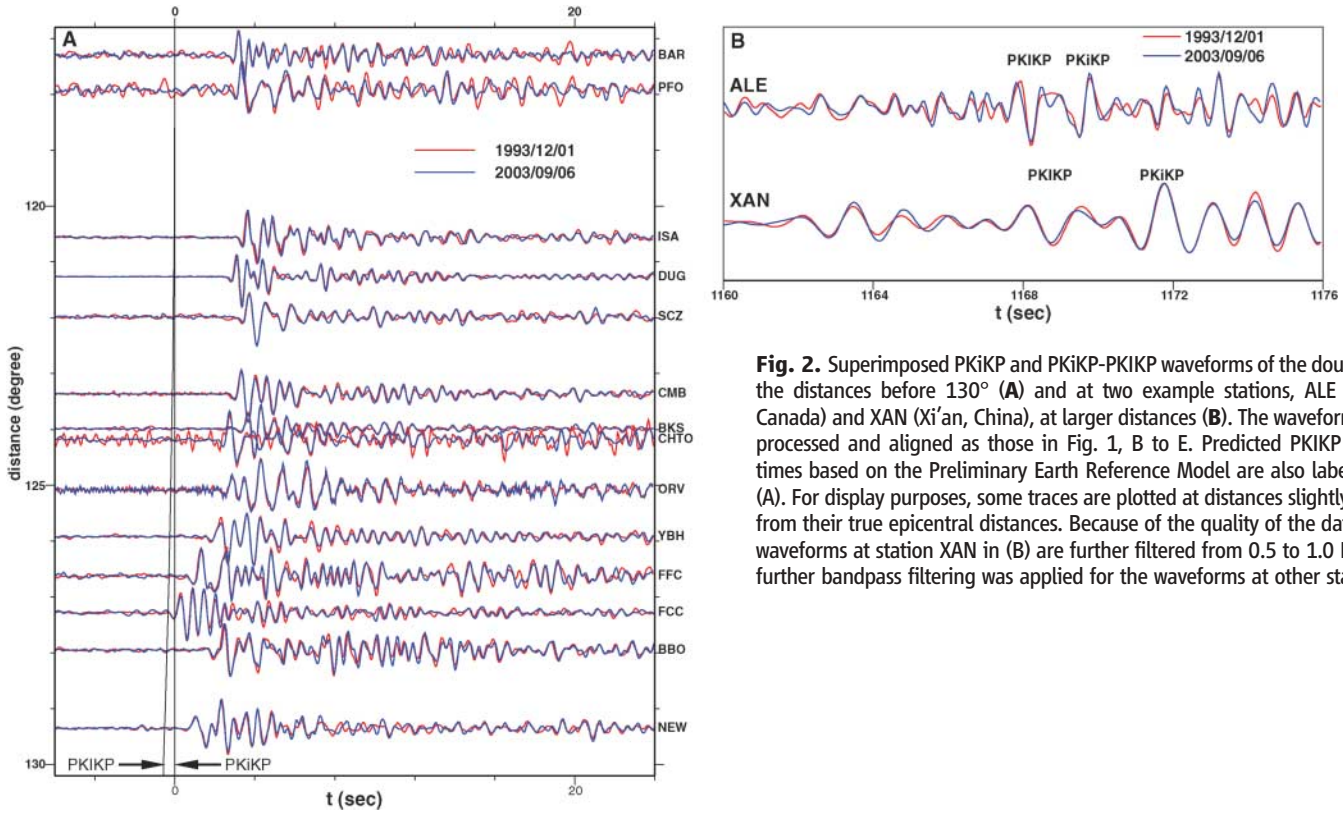

Fig. 2. Superimposed PKiKP and PKiKP-PKIKP waveforms of the doublet at the distances before 130° (**A**) and at two example stations, ALE (Alert, Canada) and XAN (Xi'an, China), at larger distances (**B**). The waveforms are processed and aligned as those in Fig. 1, B to E. Predicted PKIKP travel times based on the Preliminary Earth Reference Model are also labeled in (A). For display purposes, some traces are plotted at distances slightly away from their true epicentral distances. Because of the quality of the data, the waveforms at station XAN in (B) are further filtered from 0.5 to 1.0 Hz. No further bandpass filtering was applied for the waveforms at other stations.

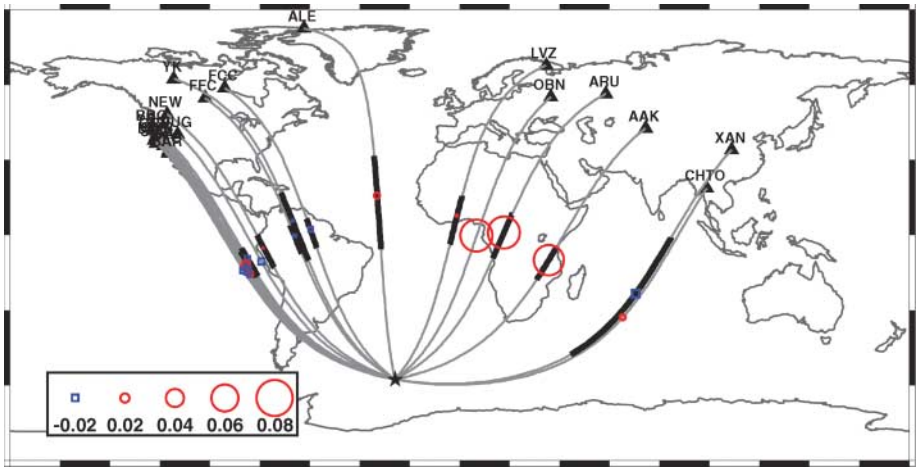

Fig. 3. Travel time residuals (*27*) of the PKiKP phases or differences in differential PKiKP-PKIKP travel time between the doublet, plotted at the reflected points of the inner core, along with the great circle paths from the doublet (star) to stations (triangles) and PKIKP ray paths in the inner core (heavy lines). Positive values indicate that the PKiKP arrives earlier or the differential PKiKP-PKIKP travel time is smaller for event 03, whereas negative values indicate the opposite. The differences in PKiKP-PKIKP differential travel time for those with heavy lines are also close to zero, except for stations ARU and AAK, in which only the differences in PKiKP-PKIKP differential travel time are shown. The great circle path to YK (Yellowknife, Canada) array comprises a total of 18 observational pairs.

graphically uniform. Furthermore, the existence of irregular topography of the inner core boundary would require the existence of small-scale variations of temperature or/and outer core composition near the inner core boundary. Because the time scale of the outer core convection is short, the required existence of small-scale variations of temperature and/or outer core composition would suggest that the rapid localized growth of the inner core is a plausible interpretation for the observed localized enlarged inner core radius. If the temporal change of the inner core boundary position is caused by rapid localized growth of the inner core, it would further suggest that the growth of the inner core and the energy release due to the solidification of the outer core are rapid and episodic. To maintain a geologically slow growth rate, the inner core growth process would also be required to be constructive for some localized regions in some time periods and destructive in other regions or in other time periods.

The above inference of the conditions near the inner core boundary would have considerable implications for the convection in the outer core and geodynamo. The inner core region with the enlarged radius corresponds to where the anomalously strong small-scale magnetic field changes in the top of the outer core are inferred at the present time (*25*) and where most of Earth's reversed magnetic polarity field has been produced in the past 400 years (*26*).

References and Notes

1. J. A. Jacobs, *Nature* **172**, 297 (1953).
2. S. I. Braginsky, *Dokl. Akad. Nauk SSSR* **149**, 1311 (1963).
3. D. Gubbins, *J. Geophys.* **43**, 453 (1977).
4. D. E. Loper, *Geophys. J. R. Astron. Soc.* **54**, 389 (1978).

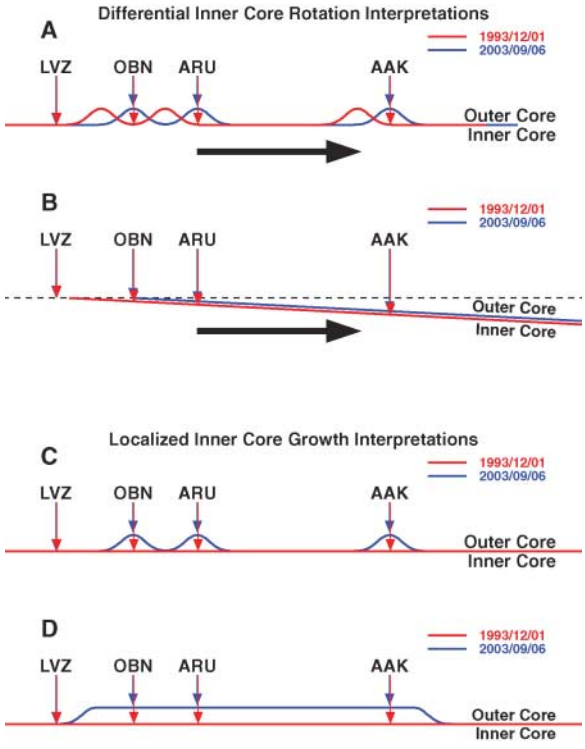

Fig. 4. Illustration of possible scenarios to change the inner core boundary at PKiKP reflected points between the occurring times of the doublet. (**A** and **B**) The inner core boundary has irregular topography and is changed by a differential inner core rotation. The dashed line in (B) is the equilibrium position of the inner core boundary. (**C** and **D**) The inner core boundary is changed by rapid localized inner core growth.

5. G. F. Davies, Paper 10/30, *XVII General Assembly. IUGG*. Canberra (1979).
6. D. E. Loper, P. H. Roberts, *Phys. Earth Planet. Int.* **24**, 302 (1981).
7. D. J. Stevenson, T. Spohn, G. Schubert, *Icarus* **54**, 466 (1983).
8. B. A. Buffett, in *Earth's Deep Interior: Mineral Physics and Tomography from the Atomic to the Global Scale*, S.-I. Karato *et al.*, Eds., Geophysical Monograph **117**, 37, American Geophysical Union, Washington, DC (2000).
9. S. Yoshida, I. Sumita, M. Kumazawa, *J. Geophys. Res.* **101**, 28085 (1996).
10. D. R. Fearn, D. E. Loper, P. H. Roberts, *Nature* **292**, 232 (1981).
11. D. J. Stevenson, *Geophys. J. R. Astron. Soc.* **89**, 311 (1987).
12. J. Zhang *et al.*, *Science* **309**, 1357 (2005).
13. G. Poupinet, A. Souriau, O. Coutant, *Phys. Earth Planet. Int.* **118**, 77 (2000).
14. G. Poupinet, W. L. Ellsworth, J. Frechet, *J. Geophys. Res.* **89**, 5719 (1984).
15. D. P. Schaff, P. G. Richards, *Science* **303**, 1176 (2004).
16. A. Y. Li, P. G. Richards, *Geochem. Geophys. Geosys.* **4**, 1072 10.1029/2004GL021240 (2003).
17. X. D. Song, *Phys. Earth Planet. Inter.* **124**, 269 (2001).
18. G. Poupinet, A. Souriau, *Phys. Earth Planet. Inter.* **124**, 275 (2001).
19. X. D. Song, P. G. Richards, *Nature* **382**, 221 (1996).
20. K. C. Creager, *Science* **278**, 1284 (1997).
21. J. E. Vidale, D. A. Dodge, P. S. Earle, *Nature* **405**, 445 (2000).
22. Materials and methods are available as supporting material on *Science* Online.
23. I. Sumita, P. Olson, *J. Geophys. Res.* **107**, 2169 10.1029/2001JB000548 (2002).
24. M. G. Worster, *J. Fluid Mech.* **237**, 649 (1992).
25. G. Hulot, C. Eymin, B. Langlais, M. Mandea, N. Olsen, *Nature* **416**, 620 (2002).
26. J. Bloxham, D. Gubbins, A. Jackson, *Philos. Trans. R. Soc. Lond. A* **329**, 415 (1989).
27. Time shifts in Fig. 1, B, D, and E, and Fig. 2, and travel time residuals in Fig. 3, are defined as $T^{pre}_{03-93,k,p}$ and $T^{res}_{03-93,k,p}$ in (*22*), respectively. They are estimated using the best-fitting relative origin time (6 September 2003, 15:47:00.205) and hypocenter position of event 03 (fig. S2A).

28. I thank two anonymous reviewers for constructive reviews and W.-C Yu for assistance in collecting the seismic data. This work is supported by the National Science Foundation.

Supporting Online Material

www.sciencemag.org/cgi/content/full/1131692/DC1
Materials and Methods
Figs. S1 to S3
Table S1
References

23 June 2006; accepted 23 August 2006
Published online 28 September 2006;
10.1126/science.1131692
Include this information when citing this paper.

Transcrystalline Melt Migration and Earth's Mantle

Pierre Schiano,[1]* Ariel Provost,[1] Roberto Clocchiatti,[2] François Faure[1]†

Plate tectonics and volcanism involve the formation, migration, and interaction of magma and gas. Experiments show that melt inclusions subjected to a thermal gradient migrate through olivine crystals, under the kinetic control of crystal-melt interface mechanisms. Exsolved gas bubbles remain fixed and eventually separate from the melt. Scaled to thermal gradients in Earth's mantle and geological times, our results account for the grain-scale segregation of primitive melts, reinterpret CO_2-rich fluid inclusions as escaped from melt, and question the existence of a free, deeply percolating fluid phase. Melt migration experiments also allow us to quantify crystal growth kinetics at very low undercoolings in conditions appropriate to many natural systems.

Deciphering the physical processes by which melts (silicate-rich liquids) and "fluids" (CO_2- or H_2O-rich gases or supercritical fluids) form, migrate, and interact is necessary to fully understand the dynamics of Earth's mantle and volcanism. It has long been believed, for instance, that the migration of magma has two modes: porous flow through small channels along grain boundaries followed by flow through a fracture network. Also, melt and fluid inclusions in mantle minerals are supposed to be the direct expressions of independent, deeply percolating fluid and melt phases (*1*). Here, we present experimental results that introduce transcrystalline melt migration as a mechanism occurring in Earth and suggest that most fluid inclusions in mantle minerals represent natural remnants of transcrystalline melt migration rather than samples of a free, fluid phase that pervades the mantle.

The samples used in this study are olivine crystals collected from lapilli levels at Piton Vincendo (Piton de la Fournaise Volcano, Reunion Island, Indian Ocean) and La Sommata

[1]Laboratoire Magmas et Volcans, Observatoire de Physique du Globe, Université Blaise Pascal et CNRS, 5 rue Kessler, 63038 Clermont-Ferrand Cedex, France. [2]Laboratoire Pierre Süe, Centre d'Etudes Nucléaires de Saclay, Commissariat à l'Energie Atomique et CNRS, 91191 Gif-sur-Yvette Cedex, France.

*To whom correspondence should be addressed. E-mail: schiano@opgc.univ-bpclermont.fr

†Present address: Centre de Recherches Pétrographiques et Géochimiques, Université Henri Poincaré et CNRS, 15 rue Notre-Dame des Pauvres, 54501 Vandoeuvre-lès-Nancy, France.

www.sciencemag.org/cgi/content/full/1131692/DC1

Supporting Online Material for

Localized Temporal Change of the Earth's Inner Core Boundary

Lianxing Wen

E-mail: wen@earth.geo.sunysb.edu

Published 28 September 2006 on *Science* Express
DOI: 10.1126/science.1131692

This PDF file includes:

Supporting Online Materials for:

Localized Temporal Change of the Earth's Inner Core Boundary

by Lianxing Wen

Materials and Methods

Seismic data

Seismic data are collected from the Global Seismographic Network, the Canadian National Seismographic Network, the Global Telemetered Seismograpic Network, The Berkeley Network, the Pacific Northwest Regional Seismic Network, the GEOSCOPE, the University of Utah Regional Seismic Network and the Trinet (Terrascope) in southern California for both events. The observed vertical components of the seismic data are used and are bandpass filtered with the WWSSN short period response. The non-IC phases used in the relocation analysis are compressional waves that include the direct wave in the mantle (P), the two branches of the seismic phases traveling in the outer core (PKPbc and PKPab), the wave reflected once off the bottom side of the core-mantle boundary (PKKPbc) and the wave scattered near the core-mantle boundary (PKP precursor). The availability of these non-IC phases provides good azimuthal coverage for relocation analysis (Fig. S1). The travel time differences of all the phases between the two events are obtained by cross-correlating the waveforms between the two events. An error of ± 0.01 s exists in such measurements. The values reported in the text took this uncertainty into account. The data time series were time interpolated to an evenly

spaced time series with a time sampling rate of 0.0025 s based on the Wiggins interpolation method *(S1)* before the cross-correlations were performed. The data interpolations are performed using the standard software package Seismic Analysis Code (SAC). PKIKP and PKiKP phases (Fig. 1a) are not used in the relocation analysis. Their arrival times and waveforms are independently checked and presented in the main text based on the relocated event parameters.

Relocation procedure

I used event 93 as the master event (i.e., fix its origin time and location to those reported in the PDE catalog, Table S1) and derive relative event location and origin time of event 03 with respect to those of event 93. For events 93 and 03, there exist these relationships:

$$T_{03,k,p} = O_{03} + t_{03,k,p} \qquad (1)$$

$$T_{93,k,p} = O_{93} + t_{93,k,p} \qquad (2)$$

where, T is the absolute arrival time of the seismic phase, O is event origin time and t is the time it takes the seismic phase to travel from the hypocenter to the station, k denotes station index, p seismic phase, *03* for event 03 and *93* for event 93. Subtracting equation (2) from (1) yields:

$$\Delta T_{03-93,k,p} = \Delta O_{03-93} + \Delta t_{03-93,k,p} \qquad (3)$$

where, $\Delta T_{03-93,k,p} = T_{03,k,p} - T_{93,k,p}$, $\Delta O_{03-93} = O_{03} - O_{93}$, $\Delta t_{03-93,k,p} = t_{03,k,p} - t_{93,k,p}$.

The above equation simply states that the difference in arrival time of seismic phase p recorded at station k between the doublet ($\Delta T_{03-93,k,p}$) equals to the difference between the origin times of the two events (ΔO_{03-93}) plus the travel time difference of the

seismic phase caused by a difference in relative hypocenter locations of the doublet ($\Delta t_{03-93,k,p}$).

$\Delta t_{03-93,k,p}$ is sensitive only to the relative location between the two events and can be expressed as:

$$\Delta t_{03-93,k,p} = dD_k * \frac{dt}{dD}(k,p,D,h) + dh * \frac{dt}{dh}(k,p,D,h) \qquad (4)$$

dD_k is the difference in epicentral distance at station k due to the relative difference in event location between the two events, $\frac{dt}{dD}(k,p,D,h)$ is the derivative of travel time of the seismic phase with respect to epicentral distance D, $\frac{dt}{dh}(k,p,D,h)$ is the derivative of travel time of the seismic phase with respect to event depth h, and dh is relative change of event depth between the two events. $\frac{dt}{dD}(k,p,D,h)$ and $\frac{dt}{dh}(k,p,D,h)$ can be calculated for each station and its associated seismic phase using a reference Earth's model. They would depend on epicentral distance D, event depth h, seismic phase p and slightly the reference model used, but exhibit little change with the absolute location and depth we assume for event 93 within their plausible error bars.

For a relative hypocenter location and a relative origin time of event 03, the predicted relative arrival time for seismic phase p recorded at station k between the doublet is defined as:

$$T^{pre}_{03-93,k,p} = \Delta O_{03-93} + \Delta t_{03-93,k,p} \qquad (5)$$

with ΔO_{03-93} being the time difference between the relative origin time of event 03 and the origin time of event 93 (fixed to the reported origin time in the PDE catalog, Table S1), and $\Delta t_{03-93,k,p}$ being the difference in travel time caused by the difference in

hypocenter location between the two events. $\Delta t_{03-93,k,p}$ is calculated based on equation (4) using the relative hypocenter location of event 03 for seismic phase *p* at station *k*.

Let $T^{obs}_{03-93,k,p}$ be the arrival time difference of seismic phase *p* recorded at station *k* and measured by cross-correlating their waveforms of the two events. For a relative location and an origin time of event 03, the travel time residual of the doublet for seismic phase *p* recorded at station *k* is defined as:

$$\Delta T^{res}_{03-93,k,p} = T^{obs}_{03-93,k,p} - T^{pre}_{03-93,k,p} \qquad (6)$$

with $T^{pre}_{03-93,k,p}$ calculated based on equation (5). Positive travel time residuals mean that, if event 03 occurs in the relative location and at the relative origin time as assumed, the seismic phase *p* at station *k* arrives later in event 03 than in event 93 even after corrected for the effects of relative hypocenter location between the two events. The negative travel time residuals indicate the opposite.

Relative location and depth for event 03 are grid-searched around the reported location and depth of event 93. The best fitting relative location, depth and origin time of event 03 are the one that generates the smallest RMS travel time residual variation defined as:

$$\sqrt{\sum_{k=1}^{N} [\Delta T^{res}_{03-93,k,p}]^2 / N} \qquad (7)$$

N is the total number of observations used in the relocation.

The above relocation technique is similar to those used to determine the relative event locations in the master event approach (e.g., *S2*-*S7*). The relative origin times of the events are also jointly inverted in the above procedures. The absolute origin times and event locations of the both events are subject to the traditional errors such as those caused by our imperfect knowledge of three-dimensional seismic structure of the Earth,

but the relative timing and event location between the doublet are not. Neither are the predictions based on equations (4), (5) and (6).

The measured $T^{obs}_{03-93,k,p}$, seismic phases, and seismic stations used in the relocation analysis are shown in Fig. S1a. The search region for the relative hypocenter location of event 03 is a 10 km (N-S direction) ×10 km (E-W direction) × 2 km (vertical) box centered at the reported location and depth of event 93. The search grid intervals are 0.002 km in N-S and E-W directions and 0.002 km in depth.

The above relocation analysis places the best-fitting relative event horizontal locations of the doublet within 0.37 km and event depths within 0.7 km (Fig. S2a). Using the Preliminary Reference Earth Model (PREM) *(S8)* and AK135 *(S9)* essentially yields same results. The best-fitting origin time for event 03 (with respect to the reported PDE origin time of event 93 in Table S1) is 2003/09/06 15:47:00.205. The relocation procedures reduce the RMS travel time residual to 0.016 s (using PREM) or 0.015 s (using AK135) for the best-fitting relative locations and origin times. The best-fitting relative location and origin time of the events also reduce the travel time residuals at each individual station between the two events (Fig. S1b). The travel time residuals of the non-IC phases in the individual stations for the best-fitting relative location and origin time range from -0.029 s (SNZO) to 0.031 s (DAWY) in the individual stations (Fig. S1b).

My relocation epicentral locations are slightly different from those obtained by Zhang et al. *(S10)*, who used a double-difference method developed by Waldhauser and Ellsworth *(S11)*. The difference is probably due to the fact that different datasets are used in the relocation analyses. The difference is small and insignificant.

RMS travel time residuals for explaining the PKiKP arrival times at ARU

While the difference in absolute PKIKP travel time observed at ARU between the doublet is just slightly above the relocation error bar, the differences in the PKiKP travel time observed at ARU, AAK and OBN between the doublet cannot be explained by a difference in event location or origin time between the doublet. I present here more analyses to show that the travel time residual of 0.11 s of the PKiKP phases between the doublet observed at station ARU cannot be explained by a difference in event location or origin time between the doublet. Same arguments can be made for the travel time shifts of the PKiKP phases observed at stations AAK and OBN.

A difference in event depth between the doublet cannot explain the data, because placing event 03 deeper to reduce the positive 0.11 s residual of the PKiKP phase at ARU would generate a similar amount of negative travel time residuals of the PKiKP and PKIKP phases at other stations. The effect of the difference in event depth is not explored further. I calculate the RMS travel time residuals and travel time residuals of the non-IC phases at each station for all possible relative event epicentral locations of event 03, by forcing the PKiKP arrival times between the doublet to fit within 0.031 s, the maximal relocation error at station DAWY in Fig. S1b. For each assumed event location of event 03, a relative origin time of event 03 is found so that the PKiKP travel time residual at ARU between the doublet (calculated based on equation (6)) is within 0.031 s. All relative event positions result in unacceptable RMS travel time residuals (Fig. S2b) and travel time residuals at many stations between the doublet (see two examples in Fig. S3). The above analysis indicates that the arrival time difference of the PKiKP phases recorded at ARU of the two events cannot be explained by a difference in event location.

Sensitivity of change of differential PKiKP-PKIKP travel time to relative event location between the doublet

The observed smaller differential PKiKP-PKIKP travel times of about 0.07 s at stations ARU and AAK in event 03 further confirm that the PKiKP travel time residuals are not caused by relative event location or origin time of the doublet. The PKiKP-PKIKP differential travel time is not affected by the earthquake origin times and is insensitive to the uncertainties of the relative location between the two events. To generate a difference of 0.07 s in PKiKP-PKIKP differential travel time, a difference of 65 km (based on PREM) or 59 km (based on AK135) in epicentral distance between the doublet is needed and a difference in PKIKP absolute travel time of 1.12 s (based on PREM) or 1.01 s (based on AK135) would result for that difference in epicentral distance. The PKiKP-PKIKP differential travel time is even less sensitive to the event depth. A change of event depth from 33 km to 0 km would only yield a difference of 0.004 s (PREM and AK135) in PKiKP-PKIKP differential travel time. All these scenarios can be excluded based on the measured arrival time differences of the two events and the relocation analysis (Figs. S1, S2a).

Effects of noise or other energy perturbation on PKiKP phase

The observed PKiKP travel time residuals at stations, ARU, AAK and OBN are not caused by noise or possible temporal changes of seismic energy proceeding the PKiKP phases. A slight ground motion unrelated to the earthquakes at a recording station, occurring at either one of the PKiKP arrival times of the doublet, may perturb the PKiKP signal. But it is highly unlikely that this would occur for all three stations with

ground motions happening to occur at the PKiKP arrival times at those stations. The PKIKP phases may generate coda waves and the coda waves may experience temporal changes (e.g., *S12, S10*). Such temporal changes of coda waves may affect the PKiKP waveforms and thus produce the apparent time shifts of the PKiKP phases at stations ARU and AAK. It is, however, a very unlikely explanation for the observed time shifts of the PKiKP phases. Note that, such PKiKP time shift is also observed at station OBN. Synthetics for all available inner core models indicate that, at an epicenter distance of stations OBN (about 123.069^{o}), the energy of the PKIKP phase is less than 4% of the PKiKP energy. The coda waves of the PKIKP phases would presumably have even less energy. The temporal changes of the PKIKP coda waves, even if they exist, would unlikely alter the PKiKP arrival times. The PKnIKP (n = 2, 3, 4 …) phases, which propagate through the inner core and are reflected off the downside of the inner core boundary *n-1* times, would arrive between the PKIKP and PKiKP phases and their possible temporal change could potentially be another source that may affect the PKiKP arrivals. But the PKnIKP phases do not appear until the epicentral distances larger than the recording distances of these stations.

Effects of temporal change of seismic properties near the hypocenters or in the mantle on PKiKP-PKIKP differential travel time

The temporal changes of travel time for the PKiKP phases recorded at stations ARU, AAK and OBN between the doublet are unlikely caused by temporal change of seismic properties near the hypocenters or in the mantle. Local temporal changes of seismic properties near the hypocenters (for example, some velocity changes due to the first event) may occur, but it would not generate the smaller PKiKP-PKIKP differential

travel time in event 03, as these two phases have almost identical take-off angles from the earthquakes (Fig. 1a). Temporal change of the seismic properties elsewhere in the mantle is unlikely. But even if it exists, the PKiKP-PKIKP differential travel times are not sensitive to the seismic structures in the mantle as they have almost identical ray paths there (Fig. 1a) *(S13, S14)*. The observed temporal changes of the PKiKP travel time recorded at ARU and AAK between the doublet are thus associated with some temporal change of the properties of the inner core boundary.

Effects of a shift of entire inner core on the change of PKiKP travel time

The localized change of inner core radius cannot be caused by a slight shift of the entire inner core toward middle Africa (the reflected points of the PKiKP phases recorded at ARU, AAK and OBN) by 0.98 - 1.75 km. A slight shift of the entire inner core would change the position of the inner core boundary elsewhere and generate PKiKP travel time difference at other stations, which is different from the observations. The PKiKP and PKiKP-PKIKP observations do not exhibit temporal change at other stations (Figs. 2, 3). A slight shift of the entire inner core would also produce similar changes of the inner core boundary position in the entry and exit points for the PKIKP phases recorded at ARU and AAK, and would generate similar amount of the travel time differences for the PKIKP phases at these two stations, and thus similar PKiKP-PKIKP differential travel times between the two events. That is also different from the observations (Figs. 1c, 1d). Thus, a localized change of inner core radius cannot be explained by a shift of the inner core.

Fresnel zone of the PKiKP waves and separation of PKiKP and PKIKP phases near the inner core boundary

For the dominant frequency of the seismic signals, the width of the Fresnel zone of PKiKP is about 150 km in the inner core boundary. This is smaller than the separation of the PKiKP and PKIKP phases at the inner core boundary, so PKiKP and PKIKP phases could respond differently to localized temporal change of inner core boundary. However, if one considers the PKIKP travel time residual of 0.04 s at ARU to be significant (which is just slightly above the relocation error bar), it is possible that the PKIKP phase at ARU is also affected by temporal change of the inner core boundary.

Temporal change of PKiKP and PKIKP coda

There is another large time shift of phase at about 4 s after the first arrivals, or about 3 s after the PKiKP phases, in the superimposed ARU waveforms (Figs. 1b,1c). This may be caused by scattering of the time-shifted PKiKP main phases by the seismic structure beneath ARU or possible temporal change of PKiKP coda waves.

The dissimilarity of the PKiKP coda waves observed at OBN, if it is attributed to the same cause for the misalignment of the PKiKP main phases, would suggest that the temporal change of topography is spatially varying to small scales. Small length scales of temporal change of inner core topography would also affect PKIKP coda waves, and may be considered as another candidate for explaining the observed temporal change of PKIKP coda waves in other studies. Different time widows of the PKiKP coda wave change are sensitive to temporal changes of different part of the inner core boundary, so the dissimilarities of the coda waves could be used to study temporal change of the inner core boundary in a large area.

Supplementary Figure Legends

Figure S1. a) Measured difference in absolute arrival time (circles and squares) of various non-IC phases used in the relocation analysis between the doublet plotted at the location of each station, along with the great circle paths (gray traces) from the doublet (star) to the stations. The arrival time differences are plotted with respect to a ΔO_{03-93} that generates a zero mean of the arrival time differences for all the stations. The circles indicate that the non-IC phases in event 03 arrive relatively earlier than their counterparts in event 93, while the squares show the opposite. Seismic stations and phases are labeled in the Figure. b) Travel time residuals $\Delta T^{res}_{03-93,k,p}$ between the doublet calculated from the measurements in a) and equations (6) and (5) using the best-fitting relative location (Fig. S2a) and origin time (2003/09/06 15:47:00.205) for event 03.

Figure S2. a) Best-fitting location of event 03 (dot labeled as 2003/09/06) relative to the location of event 93 (0,0) (star labeled as 1993/12/01) that minimizes the RMS travel time residual of the non-IC phases between the doublet, along with the RMS travel time residuals as a function of relative location of event 03. b) RMS travel time residuals of the non-IC phases as a function of relative location of event 03 by forcing the travel time residual of the PKiKP phases observed at ARU between the doublet to be within 0.031 s. Two relative locations are labeled with one that generates the minimal RMS travel time residual (dot labeled as A) and the other that produces a minimal RMS travel time residual among those that also generate a zero mean of the travel time residuals of the non-IC phases between the doublet. The travel time residuals in individual stations between the doublet in these two cases are shown in Fig. S3a and Fig. S3b, respectively.

Only the relative locations with a RMS travel time residual less than 190 ms are plotted in the figures.

Figure S3. a) Travel time residuals of the non-IC phases between the doublet for two example locations shown in Fig. S2b. Panels a and b are for the locations labeled as A and B in Fig. S2b, respectively.

Fig. S1

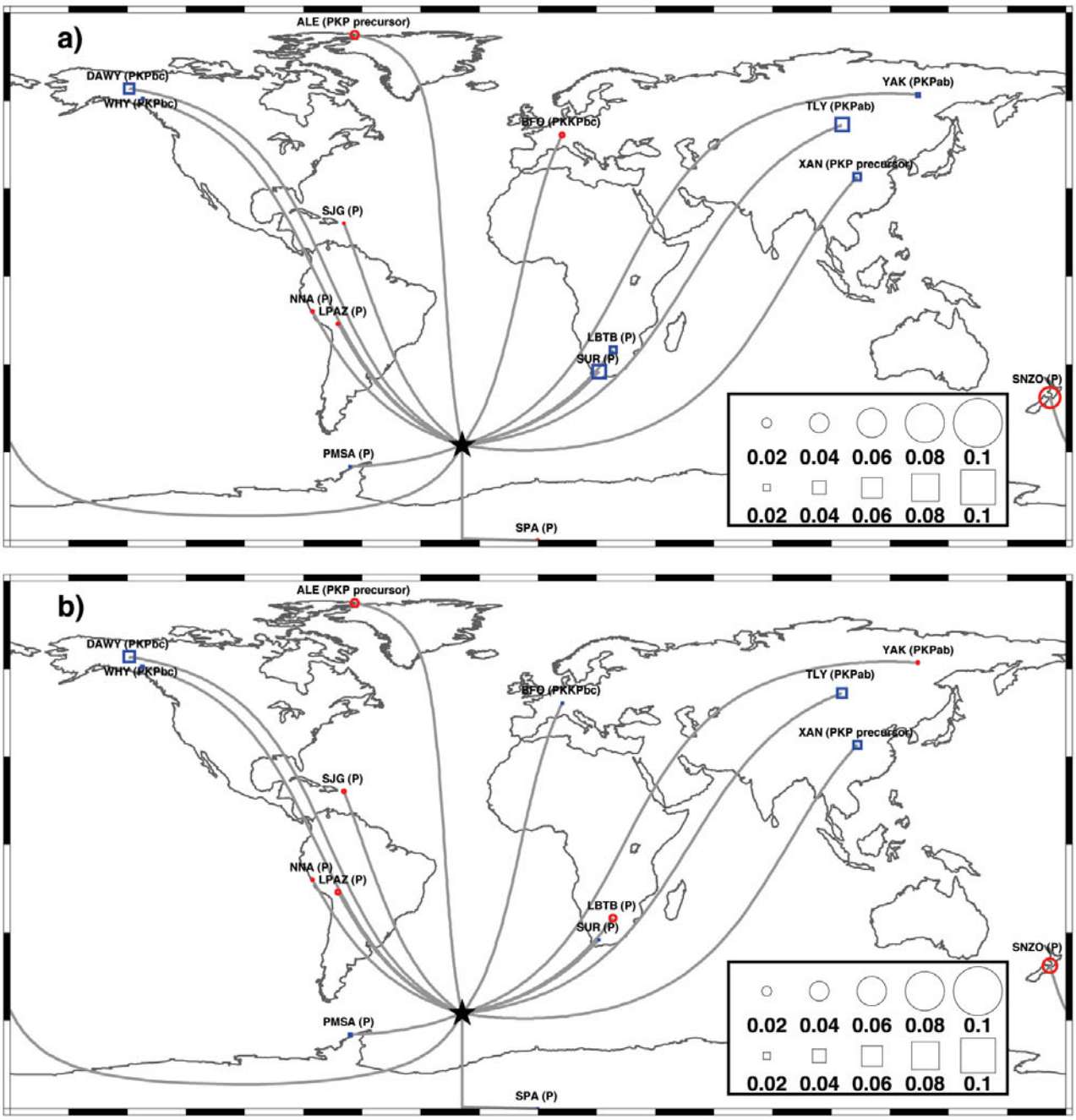
a)
ALE (PKP precursor)
DAWY (PKPbc)
WHY (PKPbc)
BFO (PKKPbc)
YAK (PKPab)
TLY (PKPab)
XAN (PKP precursor)
SJG (P)
NNA (P)
LPAZ (P)
LBTB (P)
SUR (P)
SNZO (P)
PMSA (P)
SPA (P)
0.02 0.04 0.06 0.08 0.1
0.02 0.04 0.06 0.08 0.1
b)
ALE (PKP precursor)
DAWY (PKPbc)
WHY (PKPbc)
BFO (PKKPbc)
YAK (PKPab)
TLY (PKPab)
XAN (PKP precursor)
SJG (P)
NNA (P)
LPAZ (P)
LBTB (P)
SUR (P)
SNZO (P)
PMSA (P)
SPA (P)
0.02 0.04 0.06 0.08 0.1
0.02 0.04 0.06 0.08 0.1

Fig. S2

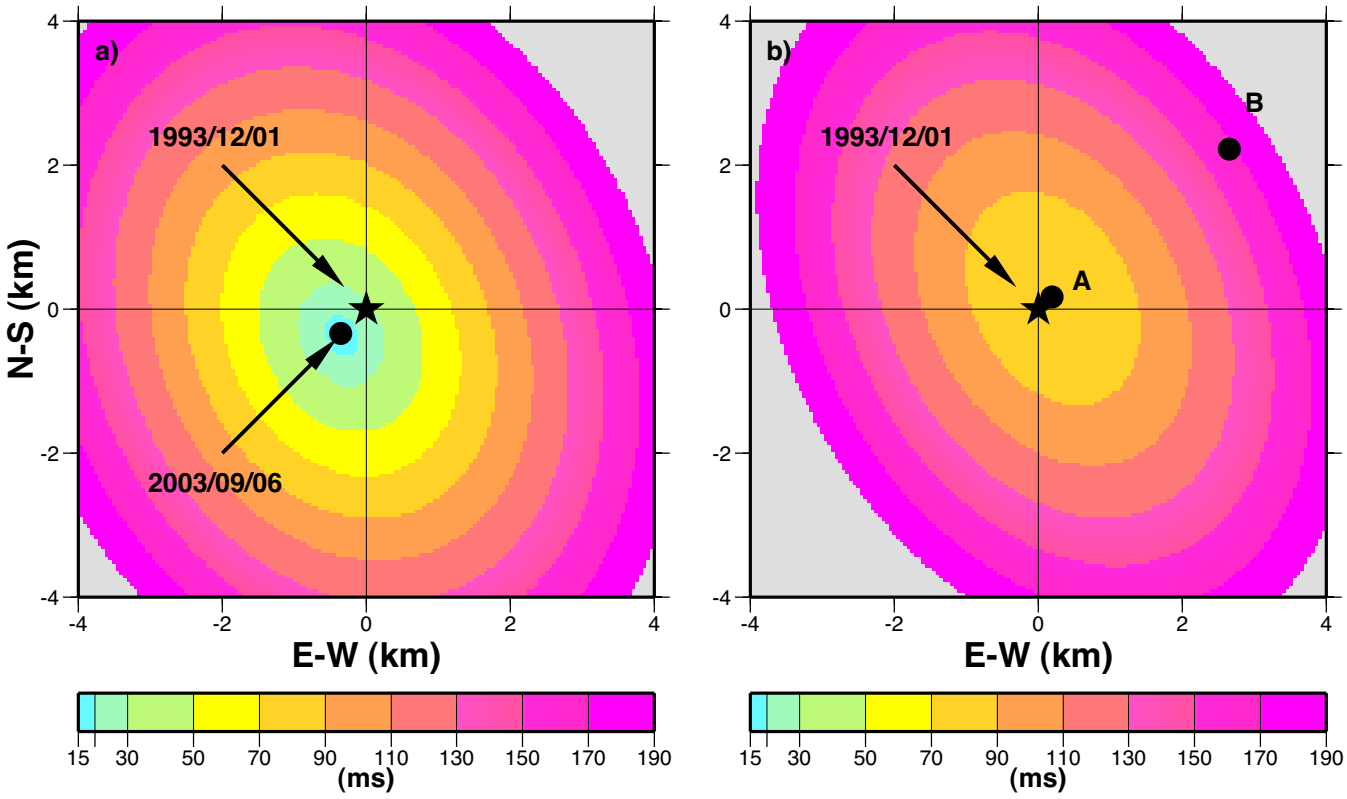
a)
1993/12/01
2003/09/06
N-S (km)
E-W (km)
4
2
0
-2
-4
15 30 50 70 90 110 130 150 170 190
(ms)
b)
1993/12/01
A
B
E-W (km)
(ms)

Fig. S3

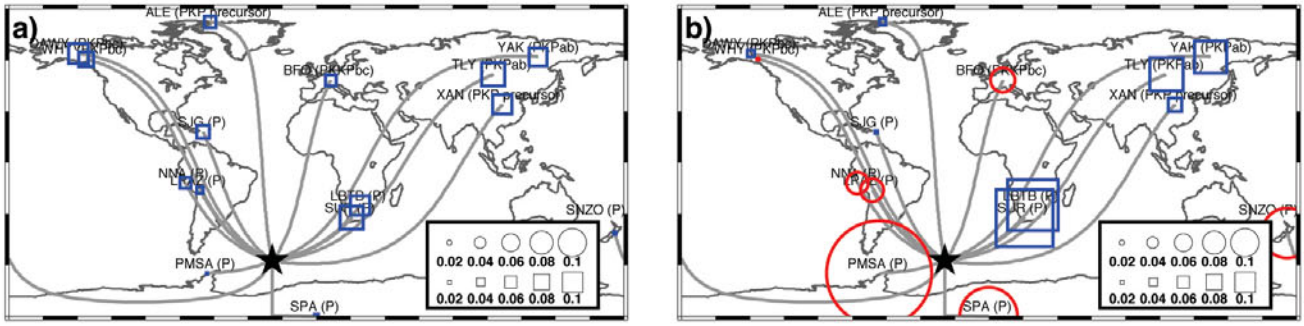
a)
ALE (PKP precursor)
YAK (PKPab)
TLY (PKPab)
XAN (PKP precursor)
SJG (P)
NNA (P)
LPAZ (P)
SNZO (P)
PMSA (P)
SPA (P)
0.02 0.04 0.06 0.08 0.1
0.02 0.04 0.06 0.08 0.1
b)
ALE (PKP precursor)
YAK (PKPab)
TLY (PKPab)
XAN (PKP precursor)
SJG (P)
NNA (P)
SNZO (P)
PMSA (P)
SPA (P)
0.02 0.04 0.06 0.08 0.1
0.02 0.04 0.06 0.08 0.1

Table S1. Event Location and Origin Time of the Doublet (PDE)

Event	Date (year/mm/dd)	Origin time (hh:mm:ss)	Latitude (^{o}N)	Longitude (^{o}E)	Depth (km)	m_b
93	1993/12/01	00:59:01.500	-57.475	-25.685	33	5.5
03	2003/09/06	15:46:59.900	-57.419	-25.639	33	5.6

References for Supporting Online Materials:

S1. R. A. Wiggins, *Bull. Seism. Soc. Am.* **76**, 2077 (1976).

S2. A. Ito, *J. Phys. Earth* **33,** 279 (1985).

S3. F. Scheberbaum, J. Wendler, *J. Geophys.* **60**, 157 (1986).

S4. M.-J. Fremont, S. D. Malone, *J. Geophys. Res.* **92,** 10223 (1987).

S5. J. C. VanDecar, R. S. Crosson, *Bull. Seism. Soc. Am.* **80**, 150 (1990).

S6. N. Deichmann, M. Garcia-Fernandez, *Geophys. J. Int.* **110**, 501 (1992).

S7. J. M. Lees, *Bull. Seism. Soc. Am.* **88**, 1127 (1998).

S8. A. M. Dziewonski, D. L. Anderson, *Phys. Earth Planet. Inter.* **25**, 297 (1981).

S9. B. L. N. Kennett, E. R. Engdahl, R. Buland, *Geophys. J. Int.* **122**, 108 (1995).

S10. J. Zhang, X. Song, Y. Li, P. G. Richards, X. Sun, F. Waldhauser, *Science* **309**, 1357 (2005).

S11. F. Waldhauser, W. L. Ellsworth, *Bull. Seism. Soc. Am.* **90**, 1353 (2000).

S12. J. E. Vidale, P. S. Earle, *Geophys. Res. Lett.* **32**, L01309, doi:10.1029/2004GL021240 (2005).

S13. F. Niu, L. Wen, *Nature* **410,** 1081 (2001).

S14. L. Wen, F. Niu, *J. Geophys. Res.* **107**, 2273, doi:10.1029/2001JB000170 (2002).